COBEM 99
XV Congresso Brasileiro de Engenharia Mecânica
15th Brazilian Congress of Mechanical Engineering
22 - 26 de Novembro de 1999 / November 22 - 26, 1999 Águas de Lindóia, São Paulo,

BUCKLING OPTIMIZATION OF COMPOSITE PLATES UNDER UNCERTAIN LOADING CONDITIONS

Alfredo R. de Faria
Jorn S. Hansen
University of Toronto - Institute for Aerospace Studies
4925 Dufferin St., Toronto, Ontario, Canada, M3H 5T6

Abstract. *Optimal elastic buckling loads of composite plates subjected to uncertain loading conditions are considered. The applied loads are not fixed during the optimization search, being allowed to vary within a certain class of admissible loads. A minimax formulation is used and the buckling loads are maximized with respect to the fiber angles and minimized with respect to applicable loading parameters which describe the set of admissible loads. The present approach has a major advantage of rendering the optimal buckling loads insensitive to perturbations in the applied loads; this is highly desirable in applications where the loads are unpredictable or varying in time.*

Keywords: *Composite Materials, Buckling, Optimization, Uncertainty*

1. INTRODUCTION

Composite materials are increasingly replacing traditional materials commonly used in structural components of aircraft and spacecraft. The motivation is mainly weight reduction and the possibility of tailoring composite laminates for very specific applications. In particular, buckling loads of structures can be increased by the use of composite materials. Moreover, the buckling loads can be maximized through a proper choice of fiber angles and/or stacking sequence.

One of the earliest works on buckling load optimization for plates was developed by Chao, Koh and Sun (1975). They show that the buckling load of a simply supported, angle-ply, symmetrically laminated rectangular plate under combined normal and shear loads can be optimized. Because of the restriction to angle-ply laminates, only one fiber angle is taken as design variable. Hirano (1979) introduced more variables to the problem by considering a general symmetric laminate with up to six layers but subjected only to axial compression. Recently, techniques related to genetic algorithms (Le Riche and Haftka, 1993) have been used to find the best stacking sequence of laminated plates which lead to optimal buckling loads.

All the aforementioned works have one point in common: the loading configuration is considered to be constant and the laminated plate is optimized to withstand only that particular configuration. This means that, if the form of the load is changed, the design will no longer be optimal and in fact the design may be extremely sensitive to such changes in load, which, in turn, constitutes a potentially hazardous situation.

Cherkaev and Cherkaeva (1998) showed that optimal designs obtained under the condition of prescribed loads are often sensitive to perturbations in these loads. This fact leads to dangerous situations where the applied loads are are allowed to vary within certain limits or, even, are unpredictable. The authors proposed a reformulation of the problem, namely, a minimax formulation, in order to eliminate the optimal design sensitivity with respect to loads.

In this work the plates to be optimized are subjected to mechanical loads which are allowed to vary. A parametrization of the mechanical loads is devised to conveniently represent the forces acting on the model and take into account its variable nature. The optimal designs thereby obtained are insensitive to changes in the loading configuration. Actually, the optimal designs are those found under the most unfavorable loading condition such that any other set of admissible loads yields larger eigenvalues (buckling loads).

2. FORMULATION OF THE PROBLEM

The objective function of the problem is the buckling load of composite plates where fiber orientations and mechanical loads are taken as design variables. The evaluation of the objective function for a particular design consists of two steps: (1) the prebuckling problem and (2) the buckling problem. Figure 1 shows the plate with applied mechanical loads and boundary conditions, assuming that the Reissner-Mindlin theory is adopted. In Fig. 1, λ is the eigenvalue associated with the buckling problem, and R_x, R_y and R_{xy} are nondimensional factors.

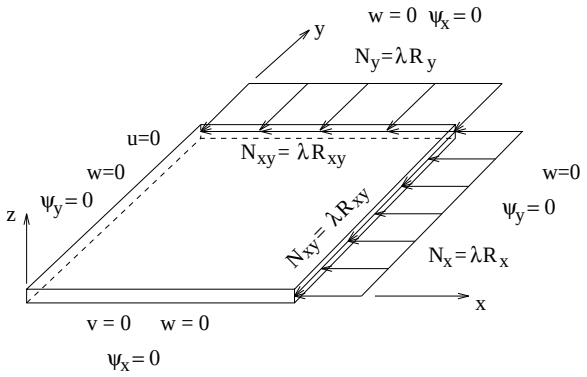

Figure 1: Plate subjected to mechanical loads and boundary conditions

The stability theory as developed by Koiter (1945) will be used in the following. Let P be the total potential energy of a structural system, $\mathbf{u}_0$ the displacements in an equilibrium state and $\mathbf{u}$ geometrically admissible displacements satisfying the boundary conditions but otherwise arbitrary. Thus, the requirement for a stable state of equilibrium is

$$P[\mathbf{u}] = P(\mathbf{u}_0 + \mathbf{u}) - P(\mathbf{u}_0) = P_1[\mathbf{u}] + P_2[\mathbf{u}] + P_3[\mathbf{u}] + P_4[\mathbf{u}] + ... \geq 0 \qquad (1)$$

where $P[\mathbf{u}]$ is the incremental total potential energy and $P_m[\mathbf{u}]$ are integrals whose integrands are homogeneous functions of order m in $\mathbf{u}$ and its derivatives. From Eq. (1) it follows that

the necessary conditions for stability of the equilibrium state $\mathbf{u}_0$ are $P_1[\mathbf{u}] = 0$ and $P_2[\mathbf{u}] \geq 0$. The relation $P_1[\mathbf{u}] = 0$ is equivalent to the principle of virtual work. The critical state is reached when $P_2[\mathbf{u}]$ is zero for a buckling mode $\mathbf{u}_1 \neq \mathbf{0}$ or, when $P_2[\mathbf{u}]$ becomes positive semi-definite. This can be written mathematically as $\delta P_2[\mathbf{u}] = 0$, where δ is the variational operator applied to $\mathbf{u}$.

Application of the stability condition in elasticity is achieved through a separation of the strain vector into a linear and a nonlinear part such that $\boldsymbol{\epsilon} = \boldsymbol{\epsilon}^L + \boldsymbol{\epsilon}^N$. Additionally, it is assumed that dead loads are applied to the structure. Thus, the total potential energy is given by

$$P(\mathbf{v}) = \frac{1}{2}\int_{\mathcal{V}} \left(\boldsymbol{\epsilon}^L(\mathbf{v}) + \boldsymbol{\epsilon}^N(\mathbf{v})\right) \cdot \mathbf{C} \cdot \left(\boldsymbol{\epsilon}^L(\mathbf{v}) + \boldsymbol{\epsilon}^N(\mathbf{v})\right) d\mathcal{V} - \int_{\Gamma} \mathbf{f} \cdot \mathbf{v} d\Gamma \tag{2}$$

where $\mathcal{V}$ is the plate volume, Γ the boundary where in-plane mechanical loads are applied and $\mathbf{C}$ the constitutive matrix. Making $\mathbf{v} = \mathbf{u}_0 + \mathbf{u}$ the expressions for $P_1[\mathbf{u}]$ and $P_2[\mathbf{u}]$ can be written as

$$\begin{aligned} P_1[\mathbf{u}] &= \int_{\mathcal{V}} \left(\boldsymbol{\epsilon}^L(\mathbf{u}_0) + \boldsymbol{\epsilon}^N(\mathbf{u}_0)\right) \cdot \mathbf{C} \cdot \left(\boldsymbol{\epsilon}^L(\mathbf{u}) + \boldsymbol{\epsilon}_1^N(\mathbf{u}, \mathbf{u}_0)\right) d\mathcal{V} - \int_{\Gamma} \mathbf{f} \cdot \mathbf{u} d\Gamma \\ P_2[\mathbf{u}] &= \int_{\mathcal{V}} \left(\boldsymbol{\epsilon}^L(\mathbf{u}_0) + \boldsymbol{\epsilon}^N(\mathbf{u}_0)\right) \cdot \mathbf{C} \cdot \boldsymbol{\epsilon}^N(\mathbf{u}) d\mathcal{V} + \\ &\quad \frac{1}{2}\int_{\mathcal{V}} \left(\boldsymbol{\epsilon}^L(\mathbf{u}) + \boldsymbol{\epsilon}_1^N(\mathbf{u}, \mathbf{u}_0)\right) \cdot \mathbf{C} \cdot \left(\boldsymbol{\epsilon}^L(\mathbf{u}) + \boldsymbol{\epsilon}_1^N(\mathbf{u}, \mathbf{u}_0)\right) d\mathcal{V} \end{aligned} \tag{3}$$

where $\boldsymbol{\epsilon}_1^N(\mathbf{u}, \mathbf{u}_0) = \boldsymbol{\epsilon}^N(\mathbf{u} + \mathbf{u}_0) - \boldsymbol{\epsilon}^N(\mathbf{u}) - \boldsymbol{\epsilon}^N(\mathbf{u}_0)$ is a bilinear and symmetric form in $\mathbf{u}$ and $\mathbf{u}_0$. Solution of $P_1[\mathbf{u}] = 0$ yields the prebuckling displacements $\mathbf{u}_0$ while the solution of $\delta P_2[\mathbf{u}] = 0$ yields the buckling mode $\mathbf{u}_1$. Because the buckling of plates is represented by a symmetric bifurcation point (Brush and Almroth, 1975), linearization of the prebuckling problem is possible such that a simplified version of $P_1[\mathbf{u}] = 0$ is written as

$$P_1[\mathbf{u}] = \int_{\mathcal{V}} \boldsymbol{\epsilon}^L(\mathbf{u}_0) \cdot \mathbf{C} \cdot \boldsymbol{\epsilon}^L(\mathbf{u}) d\mathcal{V} - \int_{\Gamma} \mathbf{f} \cdot \mathbf{u} d\Gamma = 0 \tag{4}$$

Under the assumption of linearity, the solution of Eq. (4) is given by $\mathbf{u}_0 = -\lambda \overline{\mathbf{u}}_0$, where $\overline{\mathbf{u}}_0$ is a reference state resulting from the force $\overline{\mathbf{f}}$, $\mathbf{f} = -\lambda \overline{\mathbf{f}}$ being the actual force applied to the structure (all variables associated with the reference state are identified with over-bar). Introduction of the prebuckling solution $\mathbf{u}_0 = -\lambda \overline{\mathbf{u}}_0$ into $P_2[\mathbf{u}]$ from Eq. (3) reveals that a quadratic term in λ arises because of the terms $\boldsymbol{\epsilon}_1^N(\mathbf{u}_0, \mathbf{u})$. However, simplifications can be made in $P_2[\mathbf{u}]$ if symmetric laminated plates are considered. This is because, for these plates, the prebuckling rotations and out-of-plane displacements are identically zero when only in-plane loads are applied. Thus, admitting that the Reissner-Mindlin plate theory is adopted, $w_0 = \psi_{x0} = \psi_{y0} = 0$ and the contribution of terms $\boldsymbol{\epsilon}_1^N(\mathbf{u}_0, \mathbf{u})$ are negligible. This can be clearly seen if von-Kármán theory is used since in this case the nonlinear strains depend solely on w_0. If full nonlinear strain-displacement relations are used, u_0 and v_0 are still nonzero but their contribution to the eigenproblem is minimal. Therefore, accounting for the linearity of the prebuckling state and the symmetry of the laminate, $P_2[\mathbf{u}]$ becomes

$$P_2[\mathbf{u}] = -\lambda \int_{\mathcal{V}} \boldsymbol{\epsilon}^L(\overline{\mathbf{u}}_0) \cdot \mathbf{C} \cdot \boldsymbol{\epsilon}^N(\mathbf{u}) d\mathcal{V} + \frac{1}{2}\int_{\mathcal{V}} \boldsymbol{\epsilon}^L(\mathbf{u}) \cdot \mathbf{C} \cdot \boldsymbol{\epsilon}^L(\mathbf{u}) d\mathcal{V} \tag{5}$$

3. THE FINITE ELEMENT FORMULATION

The finite element method was chosen to solve the problems $P_1[\mathbf{u}] = 0$ and $\delta P_2[\mathbf{u}] = 0$. Isoparametric bicubic Lagrangian elements with 16 nodes are used (Heppler and Hansen, 1986). These elements are known to be accurate and to eliminate shear locking effects. The Reissner-Mindlin displacements and rotations can be written in terms of nodal variables and interpolation functions as:

$$a = [\Phi] \left\{ \begin{array}{cccc} a_1 & a_2 & \ldots & a_{16} \end{array} \right\}^T \tag{6}$$

where a stands for u, v, w, ψ_x or ψ_y. Thus, the element stiffness matrix $[K]_e$ is given by:

$$[K]_e = \int_{\Omega_e} [B_\Phi]^T \left[\begin{array}{ccc} [A] & [B] & [0] \\ [B] & [D] & [0] \\ [0] & [0] & [A^*] \end{array} \right]_e [B_\Phi] \, d\Omega \tag{7}$$

where $[B_\Phi]$ are matrices which depend on the interpolation functions and its derivatives and matrices $[A]$, $[B]$, $[D]$, $[A^*]$ are the usual laminate stiffness matrices (Almeida and Hansen, 1997). Notice that the element stiffness matrix is used in both the prebuckling and the buckling problems. The element mechanical load vector, $\{f\}_e$, is

$$\{f\}_e = \lambda \int_{\Gamma_e} \left[\begin{array}{ccccc} [\Phi] & [0] & [0] & [0] & [0] \\ [0] & [\Phi] & [0] & [0] & [0] \end{array} \right]^T_{2\times 80} \left\{ \begin{array}{c} R_x + R_{xy} \\ R_y + R_{xy} \end{array} \right\} d\Gamma \tag{8}$$

Observe that the reference state, $\{\overline{f}\}_e$, is obtained by making $\lambda = -1$ in Eq. (8). The expression for $P_2[\mathbf{u}]$, given in Eq. (5), requires the knowledge of the nonlinear strain vector $\boldsymbol{\epsilon}^N$ for the Reissner-Mindlin theory. It can be found in the work of Almeida and Hansen (1997) and other publications and is of the form $\boldsymbol{\epsilon}^N = \boldsymbol{\epsilon}^N_a + z\boldsymbol{\epsilon}^N_b + z^2\boldsymbol{\epsilon}^N_c$ where z is the through the thickness coordinate. Setting $\overline{\boldsymbol{\sigma}}_0 = \mathbf{C} \cdot \boldsymbol{\epsilon}^L(\overline{\mathbf{u}}_0)$ the first integral of Eq. (5) is given by

$$\int_{\mathcal{V}} \overline{\boldsymbol{\sigma}}_0 \cdot \left(\boldsymbol{\epsilon}^N_a + z\boldsymbol{\epsilon}^N_b + z^2\boldsymbol{\epsilon}^N_c \right) d\mathcal{V} = \int_\Omega \left(\{\overline{N}_0\}^T \{\epsilon^N_a\} + \{\overline{M}_0\}^T \{\epsilon^N_b\} + \{\overline{L}_0\}^T \{\epsilon^N_c\} \right) d\Omega \tag{9}$$

where Ω is the plate middle surface domain, h is the laminate total thickness and $(\{\overline{N}_0\}$, $\{\overline{M}_0\}$, $\{\overline{L}_0\}) = \int_{-h/2}^{h/2} \overline{\boldsymbol{\sigma}}_0 (1, z, z^2) dz$ are the resultant stress moments. Because of laminate symmetry, $\overline{\sigma}_{x0}$, $\overline{\sigma}_{y0}$ and $\overline{\tau}_{xy0}$ have a symmetric distribution about $z = 0$, $\overline{\tau}_{xz0} = \overline{\tau}_{yz0} = 0$ and, consequently, $\{\overline{M}_0\}$ is identically zero. Substitution of the expressions for $\{\epsilon^N_a\}$ and $\{\epsilon^N_c\}$ into Eq. (9) gives the element geometric stiffness matrix.

$$[K_G]_e = \int_{\Omega_e} [B_{\Phi G}]^T \left[\begin{array}{ccccc} [\aleph_N] & [0] & [0] & [0] & [0] \\ [0] & [\aleph_N] & [0] & [0] & [0] \\ [0] & [0] & [\aleph_N] & [0] & [0] \\ [0] & [0] & [0] & [\aleph_L] & [0] \\ [0] & [0] & [0] & [0] & [\aleph_L] \end{array} \right] [B_{\Phi G}] d\Omega \ , \ [\aleph_F] = \left[\begin{array}{cc} \overline{F}_{x0} & \overline{F}_{xy0} \\ \overline{F}_{xy0} & \overline{F}_{y0} \end{array} \right] \tag{10}$$

where $[B_{\Phi G}]$ are matrices which depend on $[\Phi_{,x}]$, $[\Phi_{,y}]$. At this point the matrix equations for the prebuckling and buckling problems can be written as

$$[K]\{q_P\} = \{f\} \quad , \quad ([K] - \lambda[K_G])\{q_B\} = \{0\} \tag{11}$$

where $[K]$ is the global stiffness matrix, $\{q_P\}$ the prebuckling displacement vector, $\{f\}$ the global force vector, $[K_G]$ the global geometric stiffness matrix and $\{q_B\}$ the buckling mode vector.

4. OPTIMIZATION STRATEGY

Because of the periodicity of the trigonometric functions the fiber angle design variables are subjected to side constraints $-90^o \leq \theta_i \leq 90^o$, where θ_i is the orientation of the ith layer. The representation of the mechanical loads can be accomplished through the following parametrization:

$$\begin{aligned} N_x &= \lambda f_{x0} R_x = \lambda f_{x0} \left[R_{x0} + (1 - R_{x0} - R_{y0} - R_{xy0})\alpha \right] \\ N_y &= \lambda f_{y0} R_y = \lambda f_{y0} \left[R_{y0} + (1 - R_{x0} - R_{y0} - R_{xy0})\beta \right] \\ N_{xy} &= \lambda f_{xy0} R_{xy} = \lambda f_{xy0} \left[R_{xy0} + (1 - R_{x0} - R_{y0} - R_{xy0})(1 - \alpha - \beta) \right] \end{aligned} \tag{12}$$

where α and β are bounded parameters such that $0 \leq \alpha \leq 1$, $0 \leq \alpha + \beta \leq 1$, f_{x0}, f_{y0}, f_{xy0} are constant force factors and R_{x0}, R_{y0}, R_{xy0} are invariant load factors included to account for possible information on the loads available prior to the optimization. If no information is available regarding the applied loads $R_{x0} = R_{y0} = R_{xy0} = 0$; however, if for instance it is known that 50% of the loading capacity is already assigned to the load R_x, 20% to R_y and 10% to R_{xy} then $R_{x0} = 0.5$, $R_{y0} = 0.2$ and $R_{xy0} = 0.1$. In this case the 20% remaining would be distributed by the optimization procedure via parameters α, β.

The eigenvalue problem stated in Eq. (11) is solved by the subspace iteration method along with the Jacobi method to solve the projected problem (Bathe and Wilson, 1976). The least of the eigenvalues, λ_1, is the buckling load sought. It is known that optimization procedures where fiber orientations are considered as design variables often exhibit multiple optimal or near-optimal designs (Le Riche and Haftka, 1993). The multimodality of such problems implies that the optimization strategy must be chosen carefully. Classical optimization methods often converge to local optima because they move towards the optimal design closest to that where the search started, irrespective of whether this optimal design is the global optimum. In order to avoid these difficulties, probabilistic methods, which sample the entire design space (any point has a finite probability of being reached), have been used in the recent past.

The strategy implemented in this work has the capability of avoiding local optima with a certain probability, being accurate enough to provide meaningful results, and allowing the incorporation of the minimax formulation. Hence, the technique adopted consists in a combination of the attractive properties of the deterministic and probabilistic approaches. The optimization problem maximizes the buckling load under the most unfavorable loads:

$$\max_{\boldsymbol{\theta}} \min_{\boldsymbol{R}} \lambda(\boldsymbol{\theta}, \boldsymbol{R}) = \max_{\boldsymbol{\theta}} \phi(\boldsymbol{\theta}) \quad , \quad \phi(\boldsymbol{\theta}) = \min_{\boldsymbol{R}} \lambda(\boldsymbol{\theta}, \boldsymbol{R}) \tag{13}$$

where $\boldsymbol{\theta}$ is the vector of fiber angle design variables, $\boldsymbol{R}$ the vector of load parameters and ϕ a new objective function. Thus, the minimax problem is reduced to a maximization problem where the objective function is itself a minimization problem.

5. NUMERICAL SIMULATIONS

The proposed strategy is used to simulate two plates with aspect ratios of $a : b = 1 : 1$ and $a : b = 2 : 1$ both with five composite plies of equal thickness. All plates simulated have sides $a = 360$ mm or $a = 720$ mm and $b = 360$ mm, depending on the aspect ratio, laminate thickness of 0.6 mm and are free of initial imperfections. The assumption of a perfectly flat

plate is reasonable because the loss of stability of such structures is not catastrophic since its bifurcation point is symmetric and the secondary path does not drop downward after the critical load is reached (Brush and Almroth, 1975). The boundary conditions for the prebuckling and buckling problems are illustrated in Fig. 1.

As mentioned, two steps are necessary to evaluate the objective function for a particular design. The step which requires the most intense computational effort is by far the buckling problem calculation (step 2). Thus, every attempt to improve efficiency of step 2 is worthwhile. Significant improvement without serious loss of accuracy can be achieved as follows: instead of considering the complete model with u, v, w, ψ_x and ψ_y, assume that u and v make a negligible contribution to the eigenvalue problem. In this way the eigenvector associated with the simplified model contains only components related to w, ψ_x and ψ_y. Comparison between the complete model and the simplified model reveal differences of less than 0.3% in the buckling load.

The material chosen for simulation is graphite/epoxy T300-5208; its properties are available in the work by Adams, Bowles and Herakovich (1988) and, for a temperature of 21^oC, are: $E_{11} = 154.5$ GPa, $E_{22} = 11.13$ GPa, $\nu_{12} = 0.304$, $G_{12} = G_{13} = 6.98$ GPa and $G_{23} = 3.36$ GPa. The parameters associated with the genetic algorithm (GA) implemented are: population size of 100 individuals, 97% of probability of cross-over and 50% of probability of mutation. Each design is encoded as a string (chromosome) of genes, each which representing the fiber orientations and whose alleles range from -90^o to $+90^o$. The cross-over process is implemented by randomly selecting a break point in two parents' chromosomes and exchanging substrings in order to generate the off-spring. Then, mutation may occur with a probability of 50% per chromosome. One gene is randomly chosen in the child's chromosome and it is assigned an angle within the range of alleles. An elitist strategy is adopted such that the best fitted individual of a generation is cloned to the next generation. This strategy provides a useful stopping criterion: the search is assumed to have converged if the best design remains unchanged for 5 generations. In this work, 2×2 (square) or 2×4 (rectangular) finite element meshes are implemented in all optimization calculations using the genetic algorithm method. A typical run of the GA takes 5,000 function calculations (λ evaluations).

The genetic algorithm handles the maximization problem while the evaluation of the reduced objective function ϕ from Eq. (13) is achieved through Powell's method. The first approximation of the optimal design obtained by the GA is refined using Powell's method. This time both the maximization and the minimization problems are solved through Powell's method. Typically 1,000 objective function evaluations are needed for convergence.

5.1 Square Plate

The plate sides are $a = b = 360$ mm and the laminate is $[\theta_1/\theta_2/\theta_3/\theta_2/\theta_1]$. Hence, the number of fiber angle design variables is three. Eleven load cases are considered. The first three correspond to the traditional optimization under constant loads: $R_{x0} = 1.0$ (case 1), $R_{y0} = 1.0$ (case 2) and $R_{xy0} = 1.0$ (case 3). For simulation purposes it was admitted that 75% of the loading capacity is constant during the optimization and is distributed between R_{x0}, R_{y0} and R_{xy0} in seven load cases: $R_{x0} = 0.75$ (case 4), $R_{y0} = 0.75$ (case 5), $R_{xy0} = 0.75$ (case 6), $R_{x0} = R_{y0} = 0.375$ (case 7), $R_{x0} = R_{xy0} = 0.375$ (case 8), $R_{y0} = R_{xy0} = 0.375$ (case 9), $R_{x0} = R_{y0} = R_{xy0} = 0.25$ (case 10). Additionally, the most general case where no previous information on the loads is available ($R_{x0} = R_{y0} = R_{xy0} = 0.0$, case 11) is also simulated in order to offer some insight into the minimax formulation.

Table 1 presents the results for the optimized square plate. Load cases 1, 2, 3 are obtained making $f_{x0} = 1.0$, $f_{y0} = 1.0$, $f_{xy0} = 1.0$. The remaining load cases are then obtained making f_{x0}, f_{y0}, f_{xy0} equal to the optimal forces previously found for cases 1, 2, 3, respectively. For the particular square plate under investigation $f_{x0} = f_{y0} = 407.4$ N/m (cases 1 and 2), $f_{xy0} = 594.1$ N/m (case 3). In all simulations a 2×2 finite element mesh is used to model the full square plate. Comparison with the 3×3 finite element mesh reveals that the buckling loads obtained with the 2×2 mesh have converged. The last column of Table 1 refers to the number of objective function evaluations needed for convergence.

Table 1 - Optimization for square plate

case	θ_1	θ_2	θ_3	R_x	R_y	R_{xy}	λ_1	No.
1	-44.7	44.9	46.2	1.000	0.000	0.000	1.000	2080
2	-45.4	45.1	43.4	0.000	1.000	0.000	1.000	1783
3	65.4	9.2	9.2	0.000	0.000	1.000	1.000	991
4	43.3	-48.1	-86.7	0.750	0.000	0.250	0.928	3711
5	46.0	-45.7	85.4	0.000	0.750	0.250	0.927	4054
6	26.5	83.9	82.3	0.250	0.000	0.750	0.928	9429
7	45.7	-42.5	-0.2	0.375	0.375	0.250	0.928	5488
8	39.6	-79.4	89.7	0.625	0.000	0.375	0.881	5992
9	50.7	-9.1	0.6	0.000	0.625	0.375	0.879	6186
10	43.9	-75.3	89.4	0.250	0.250	0.500	0.880	2610
11	44.0	-78.3	87.4	0.000	1.000	0.000	0.832	2213

Observe that the plate is square and the boundary conditions are symmetric about the diagonal passing through the origin of the reference system of Fig. 1. Thus, provided there is symmetry in the loading conditions, symmetric designs about the diagonal should be obtained. This symmetry can be readily verified in the pairs of load cases 4 and 5, and 8 and 9. In these cases, the two designs, 4 and 5 or 8 and 9, yield (nominally) identical buckling loads and the optimal fiber angles involve (effectively) a 90^o rotation. In order to simplify the notation, we introduce λ_1^i meaning λ_1 obtained by the minimax formulation for load case i.

Through investigation of load case 6, it is possible to verify the existence of two optimal designs appearing because of the diagonal symmetry. Taking load case 6, it is seen that the optimal design possesses $R_x = 0.25$, $R_y = 0.0$, $R_{xy} = 0.75$ and $\lambda_1^6 = 0.928$. The same design loaded with $R_x = 0.0$, $R_y = 0.25$ and $R_{xy} = 0.75$ yields $\lambda_1^3 = 0.932$ which is very close to the original 0.928.

It is interesting to compare load cases 1, 2 and 3 with 4, 5 and 6, respectively. As expected, λ_1^1 is greater than λ_1^4, λ_1^2 is greater than λ_1^5 and λ_1^3 is greater than λ_1^6. However, if the load ratios are varied, the optimal design obtained under constant loads perform poorer. For example, if the optimal design obtained for case 3 is loaded with $R_y = 1$, it gives only $\lambda_1 = 0.699$ but, if the optimal design obtained for case 11 is loaded with $R_y = 1$, it gives $\lambda_1 = 0.832$.

5.2 Rectangular Plate

The laminated plate to be considered has sides $a = 360$ mm and $b = 540$ mm and the laminate is $[\theta_1/\theta_2/\theta_3/\theta_2/\theta_1]$. For this plate there is no diagonal symmetry such as in the square plate and therefore no comparison between load cases 3 and 4, and 8 and 9 is possible. Table 2 presents the results for the optimized nonuniform single-ply plate. Load cases 1, 2,

3 are obtained making $f_{x0} = 1.0$, $f_{y0} = 1.0$, $f_{xy0} = 1.0$. The remaining load cases are then obtained making f_{x0}, f_{y0}, f_{xy0} equal to the optimal forces previously found for cases 1, 2, 3, respectively. For the particular rectangular plate under investigation $f_{x0} = 246.0$ N/m (cases 1), $f_{x0} = 431.4.0$ N/m (cases 2), $f_{xy0} = 344.2$ N/m (case 3). In all simulations a 2×3 finite element mesh is used to model the full plate.

Table 2 - Optimization for rectangular plate

case	θ_1	θ_2	θ_3	R_x	R_y	R_{xy}	λ_1	No.
1	-5.0	24.8	23.7	1.000	0.000	0.000	1.000	3001
2	-48.7	46.7	43.2	0.000	1.000	0.000	1.000	2672
3	66.0	3.1	74.9	0.000	0.000	1.000	1.000	7607
4	-4.6	23.0	23.7	1.000	0.000	0.000	0.999	4694
5	47.3	-35.7	-9.5	0.000	0.750	0.250	0.990	10492
6	59.1	-10.4	71.5	0.000	0.250	0.750	0.957	5753
7	27.5	-33.1	61.5	0.375	0.625	0.000	1.020	7234
8	39.4	-22.5	-9.1	0.375	0.000	0.625	1.030	10066
9	43.0	-35.2	-6.9	0.000	0.375	0.625	0.944	4875
10	42.7	-24.0	-5.6	0.250	0.250	0.500	1.027	8149
11	38.9	-34.2	-5.9	1.000	0.000	0.000	0.871	7123

Similarly to the square plate, comparison between load cases 1 and 4, 2 and 5 or 3 and 6 reveals that $\lambda_1^1 > \lambda_1^4$, $\lambda_1^2 > \lambda_1^5$ and $\lambda_1^3 > \lambda_1^6$. Nevertheless, if the loads are varied, the optimal design obtained under uncertain loading conditions have a superior performance. For example, if the optimal design obtained for case 2 is loaded with $R_x = R_y = R_{xy} = 1/3$ it gives only $\lambda_1 = 0.829$ but if the optimal design obtained for case 11 is loaded with $R_x = R_y = R_{xy} = 1/3$ it gives $\lambda_1 = 1.037$.

A direct comparison between the two optimal design can be visualized in Fig. 2a where the ratio $\lambda_1^{11}/\lambda_1^2$ is plotted for various loading configurations. The region where design 2 performs better ($\lambda_1^{11}/\lambda_1^2 < 1$) corresponds to the neighborhood of $\alpha = 0$, $\beta = 1$ ($R_x = R_{xy} = 0$, $R_y = 1$). Away from this region, design 11 becomes better ($\lambda_1^{11}/\lambda_1^2 > 1$). This behavior is understandable because the optimal design obtained for case 2 is specifically tailored to withstand the load $R_x = R_{xy} = 0$, $R_y = 1$. Approximately, $\lambda_1^{11}/\lambda_1^2 > 1$ in 82% of all the loading situations.

6. COMMENTS

The numerical results obtained confirm that plates optimized under uncertain loads deliver a better overall performance than those optimized under constant loads. The mechanical load sensitivity of the traditionally optimized plates can be compensated by a reformulation of the problem to take into account the variable nature of the loads. It is to be noted that an increase in certainty in the specification of the loading configuration prior to the optimization process leads to increases in the optimal buckling loads, however, such designs are inferior for loads other than the design loads.

It is possible to plot the design space related to parameters α and β from Eq. (12) for the optimal designs obtained and verify that the buckling load found through the minimax formulation actually corresponds to a minimum with respect to these parameters. In order to illustrate this, the design space of the mechanical loads for the rectangular plate and load case 11 is plotted in Fig. 2b. No local minima are present in Fig. 2b and, in accordance with Table 2, the minimum point is found for $\alpha = 1$ and $\beta = 0$ which corresponds to $R_y = R_{xy} = 0$

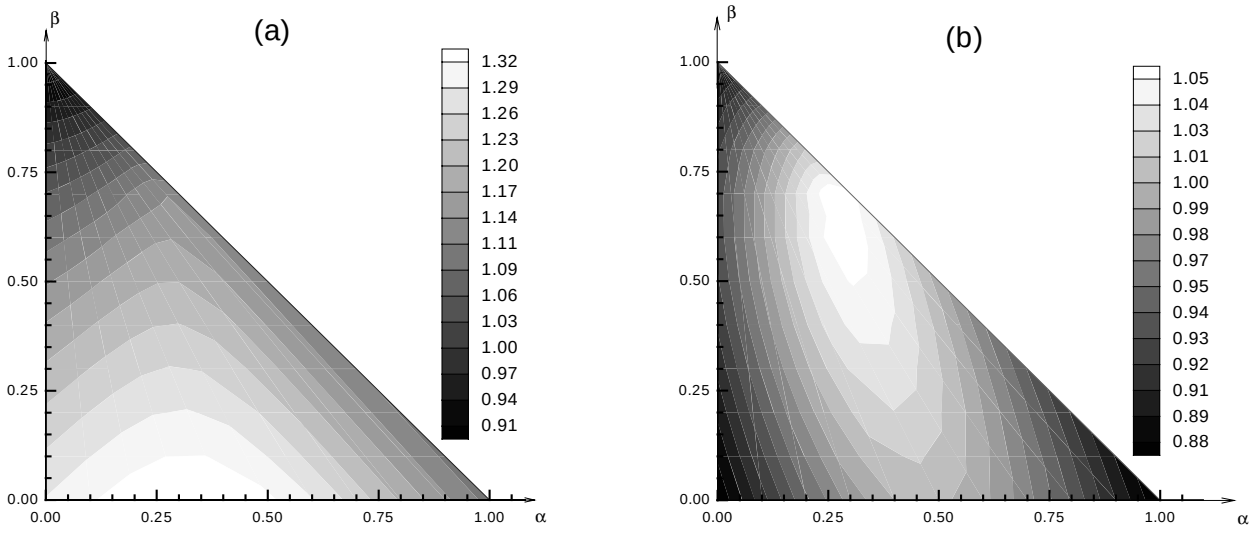

Figure 2: Comparative performance and design space of mechanical loads

and $R_x = 1$. Notice also that the loads $R_x = R_{xy} = 0$, $R_y = 1$, and $R_x = R_y = 0$, $R_{xy} = 1$ also give $\lambda_1 = 0.871$.

A study is conducted to assess the effect of the degree of uncertainty on the optimal designs obtained through the minimax formulations for the square and rectangular plates. Maintaining $R_{y0} = R_{xy0} = 0.0$, five situations are considered ($R_{x0} = 0.0$, 0.25, 0.50, 0.75 and 1.00) and the result is shown in Fig. 3.

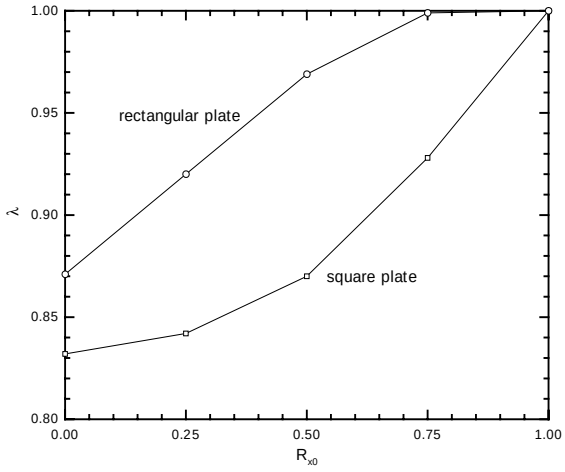

Figure 3: Effect of uncertainty degree on the optimal buckling load

The ideas introduced in this work regarding the minimax formulation applied to uncertain mechanical loads in composite laminated plates can be extended to other composite structures. Cylindrical shells, which exhibit a catastrophic buckling behavior, could benefit from the techniques presented here and are the subject of ongoing work.

Acknowledgements

This work was supported by CAPES and the NSERC (operating grant No. 3663).

REFERENCES

Adams , D.S., Bowles, D.E. and Herakovich, C.T., 1988, Thermally induced transverse cracking in graphite-epoxy cross-ply laminates, *Environmental effects on composite materials*, Vol. 3, ed. Springer, Technomic Publ. Co. Inc., Lancaster, Pennsylvania, pp. 247-274.

Almeida, S.F.M. and Hansen, J.S., 1997, Enhanced elastic buckling loads of composite plates with tailored thermal residual stresses, *Journal of Applied Mechanics*, Vol. 64, pp. 772-780.

Bathe, K-.J. and Wilson, E.L., 1976, Numerical methods in finite element analysis, Prentice Hall Inc., New Jersey.

Brush, D.O. and Almroth, B.O., 1975, Buckling of bars, plates and shells, McGraw-Hill Inc., New York.

Chao, C.C., Koh, S.L. and Sun, C.T., 1975, Optimization of buckling and yield strengths of laminated composites, *AIAA Journal*, Vol. 13, No. 9, pp. 1131-1132.

Cherkaev, A. and Cherkaeva, E., 1998, Stable optimal design for uncertain loading conditions, submitted to *Homogenization*, *World Scientific*, edited by V. Berdichevsky.

Heppler, G.R. and Hansen, J.S., 1984, A Mindlin element for thick and deep shells, *Computer Methods in Applied Mechanics and Engineering*, Vol. 54, No. 1, pp. 21-47.

Hirano, Y., 1979, Optimum design of laminated plates under axial compression, *AIAA Journal*, Vol. 17, No. 9, pp. 1017-1019.

Holland, J.H., 1975, Adaptation in natural and artificial systems, *The University of Michigan Press*, Ann Arbor, MI.

Koiter, W.T., 1945, On the stability of elastic equilibrium (in Dutch with English summary), thesis, Delf, H. J. Paris, Amsterdam. English translation, *Air Force Flight Dyn. Lab. Tech.*, report AFFDL-TR-70-25, February, 1970.

Le Riche, R. and Haftka, R.T., 1993, Optimization of laminate stacking sequence for buckling load maximization by genetic algorithm, *AIAA Journal*, Vol. 31, No. 5, pp. 951-956.

Vanderplaats, G.N., 1984, Optimization techniques for nonlinear engineering design with applications, McGraw-Hill, New York.